

Modular Wi-Fi Sensor Node for Indoor Environmental Sensing Applications

Philipp Bolte

Dept. of Electronics and Circuit Technology
South Westphalia University of Applied Sciences
Soest, Germany
e-mail: bolte.philipp@fh-swf.de

Ulf Witkowski

Dept. of Electronics and Circuit Technology
South Westphalia University of Applied Sciences
Soest, Germany
e-mail: witkowski.ulf@fh-swf.de

Abstract—A wireless sensor node with Wi-Fi interface has been developed and applied to measure air quality parameters. The node can be used for different indoor sensing applications, but the currently addressed application context is to reduce the risk of virus infection that is related to the aerosol concentration in a room. As a helpful measure, the carbon dioxide (CO₂) concentration can be considered because there is a relation between CO₂ concentration and aerosol concentration. Two different approaches of CO₂ measurements, direct and indirect, are tested. Captured data is wirelessly transmitted via Wi-Fi to a database for detailed analysis. By using multiple sensor nodes, a spatial distribution of CO₂ can be calculated by using the inverse distance weighting interpolation technique. The resulting CO₂ distribution data can be used to optimize the number of required sensor nodes for a specific room and their placements. Another aspect is the dynamics of the CO₂ concentration when ventilating the room, e.g., by opening windows to reduce the aerosol concentration in a room. A single sensor node or multiple nodes can be used to set up an alarm system that indicates pending room ventilation in case of high CO₂ concentration. A set of five sensor nodes have been installed into a small room to record CO₂ concentration over time with a closed window and when airing the room.

Keywords—Wireless sensor; Distributed sensing; CO₂ concentration measurement; Aerosol distribution

I. INTRODUCTION

Virus diseases like the pandemic Covid-19 require multiple approaches to reduce the number of infections. One approach is to filter infectious particles by optimized filter systems in indoor scenarios but these systems can be difficult and expensive to install. Another approach is to apply regular room ventilation to reduce virus concentration. To optimize this process, a measure can be helpful to identify the virus concentration. For Covid-19 there is an expected relation between virus concentration of SARS-CoV-2 in the air and the aerosol concentration because viruses are usually connected to aerosols emitted during human's breathing and speech. But to directly measure the aerosol concentration is difficult. It is much simpler to measure the carbon dioxide (CO₂) concentrations instead because current research has shown a correlation between aerosol and CO₂ concentrations [1]. Retrofitting existing buildings with modern Heating, Ventilation and Air Conditioning (HVAC) systems incorporating automatic ventilation is a challenging task [2]. The extensive use of CO₂ sensors in classrooms and offices without automatic HVAC systems could improve the ventilation habits and therefore reduce the CO₂ concentration and consequently

the concentration of potentially virus-contaminated aerosols. CO₂ sensors and related measurement systems can be easily deployed in indoor scenarios. But it is usually necessary to install more than a single sensor at different positions in a room to get a realistic view of the CO₂ concentration and distribution in order to optimize ventilation frequency and duration.

We propose a modular Sensor Node (SN) that enables the deployment for different scenarios. The SN is built around the self-designed IoTyze Wi-Fi module. A Nondispersive Infrared (NDIR) CO₂ and a Volatile Organic Compounds (VOC) sensor can be connected to the SN. The gathered data from the connected sensors is buffered and transmitted via the Message Queuing Telemetry Transport (MQTT) protocol using a Wi-Fi modem every 30 seconds. One use case is the local display of the measured air quality parameters to support the regular airing of the room. A display is connected to show the air quality parameters. An optical and acoustical alert is triggered if the air quality parameters reach a critical limit to indicate the need for ventilation. The measured data is stored in a database as evidence.

For a second application, a network of multiple SN is deployed to measure the indoor spatial CO₂ concentration. The spatial CO₂ concentration in classrooms is not uniformly distributed, it depends on room geometry as well as on the type of ventilation [3]. Experiments have shown that the CO₂ concentration in occupied space can be estimated using computational fluid dynamics (CFD) simulation if the boundary conditions are known [5]. The concept was only applied to simple room geometries. A network of multiple SN could be used to experimentally determine the optimal location for a single CO₂ sensor inside complex structured rooms (e.g., classrooms with many tables and chairs) without the need for complex CFD simulations. This paper proposes a method for interpolating the CO₂ concentration measurements that is tested with preliminary data recorded in home office.

The paper is organized as follows: In Section 2 the architecture of the developed sensor node is described. This includes hardware components, integrated sensors for CO₂ measurement, and the data flow for storing the sensor data in a database. The interfaces to access the sensor data locally or remote via online display are introduced in Section 3. Also comparisons are made for direct and indirect measurement of CO₂ concentration. Data analysis and spatial interpolation is explained in Section 4. Section 5 concludes the paper.

II. SENSOR NODE ARCHITECTURE

We propose the use of the IoTyze Wi-Fi board as the main controller for the SN. This board combines a powerful STM32 Microcontroller (MCU), an ESP32 Wi-Fi System on Chip (SoC) and additional periphery, as shown in Figure 1. One of the sensors or both, i.e., SCD30 and BME680, can be connected to the board. The display unit is an optional feature if a local display is required. The IoTyze ecosystem provides a software framework with a variety of different sensor drivers and an easy-to-use file-based device configuration via USB flash-drive emulation [4]. The use of a Wi-Fi modem supports high transmission rates but requires an external power supply. The LoRaWAN and LTE NB-IoT variants are not used because of the limited bandwidth. A battery-supplied operation is not considered because of the high current consumption of the used sensors due to continuous measurements. The use of a USB power supply for the sensor nodes is not a problem anyway since the SNs are placed indoor at a fixed position.

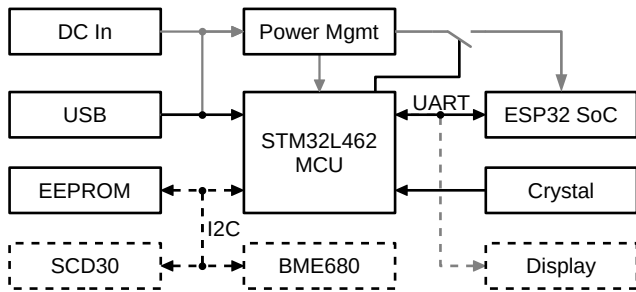


Fig. 1. Hardware block diagram of the sensor node

A. Hardware

The IoTyze Wi-Fi board integrates an STM32L462 host processor and an ESP32 SoC that executes the TCP/IP stack. The communication between the host processor and the Wi-Fi module is established using UART with a baud rate of 115200 bit/s. External oscillators are connected to the host processor to provide precise timing. An I²C EEPROM is used for storing the device configuration and status data. A micro USB port is used to access the device configuration and for the power supply. The board can also be supplied by using a DC connector. The power rails, GPIOs, UART-, I²C- and SPI-interfaces from the host processor are available through a 20 pin header. The sensors, including the optional display, are connected to the controller board using this connector.

B. Air Quality Sensors

The main sensor device to estimate the aerosol concentration is the Sensirion SCD30 sensor to measure the CO₂ concentration because of the correlation between CO₂ concentration and aerosols. Furthermore, this sensor also measures temperature and humidity. The device is connected to the host processor using the I²C bus. The measurement of the CO₂ concentration is based on NDIR principles. The sample gas is irradiated by a wideband light source and two photosensors with specific

passbands that measure the difference of a wavelength of 4.3 μm, that is attenuated by CO₂ molecules, compared to a wavelength of 4 μm, that is minimally absorbed by air gases [6]. CO₂ concentrations between 0 parts per million (ppm) and 40000 ppm can be measured and the accuracy is specified by 30 ppm or 3% [7]. The direct measurement of CO₂ concentration with an NDIR sensor is fairly expensive.

Furthermore, the SN can be equipped with a Bosch BME680 VOC sensor. This sensor integrates four different sensing principles for gas, humidity, pressure and temperature. It has been optimized for IoT, home automation and control and other applications. The VOC sensing is based on proven sensing principles, i.e., depending on the type of gas that is flowing along a heated metal-oxide surface different resulting conductivities could be electrically measured [8]. A survey of students has shown that the indoor comfort satisfaction of students does not exclusively depend on CO₂ concentration and that other micro-climate factors (e.g., temperature, humidity, smell) must also be taken into account [9]. The hotplate sensors measure a wider range of VOC pollutants, e.g., outgassing from garbage, paint and furniture that is processed by the integrated Bosch BSEC sensor fusion which outputs the CO₂ equivalent based on the correlation of VOC and CO₂ concentrations in humans exhaled breath [10]. The data from the sensor fusion of the BME680 measurements can be used as additional air quality parameters.

C. Data Flow

The proposed SN reads data from the connected sensors and performs the required data preprocessing for transmission of the buffered measurements as shown in Figure 2.

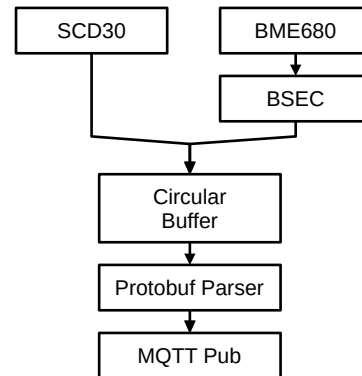


Fig. 2. Internal data flow of the sensor node

The CO₂ concentration, temperature and humidity readings from the SCD30 sensor with a sampling period of 2 seconds are directly transferred into a circular FIFO buffer. The data from the BME680 is processed by the proprietary Bosch Sensortec Environmental Cluster (BSEC) sensor fusion library [11]. The BSEC sensor fusion outputs virtual sensor values for temperature, humidity, ambient pressure, Indoor Air Quality (IAQ) and CO₂ equivalent with a sampling period of 3 seconds that is stored in the circular FIFO buffer. The circular FIFO buffer is implemented around a nested C structure that is

generated by the Nanopb compiler from a payload description [12]. The FIFO buffer is converted into the binary protocol buffers data format using the Nanopb encoder. The binary payload is transferred by a publish message using the MQTT protocol. For the proposed sample application, the payload is decoded and stored into an InfluxDB database by a Node-RED instance. The data can be exported to a CSV formatted text file for further processing and analysis.

III. AIR QUALITY DISPLAY

For the first application, the SN was equipped with a display and a buzzer, as shown in Figure 3. The hardware is placed inside a 3D printed case. The sensors are located at the back of the case. An air-permeable cap is used as mechanical protection. The device is supplied by an external 5V power supply with a standard micro USB connector. The software was developed for use with both, the SCD30 CO₂ and the BME680 VOC sensor, but also works with one of the sensors, lacking the values of the disconnected device.



Fig. 3. Fully equipped sensor node

A. Local Display

The measured environmental parameters from the SCD30 sensor and the BSEC sensor fusion are additionally fed into an air quality state management software module. This module classifies the air quality based on the last CO₂ reading, the IAQ estimation and the assessments of the standard DIN EN 13779 [13]. The standard refers to CO₂ concentrations above the ambient level for classification. The globally averaged CO₂ concentration for the year 2019 was 410.5 ppm [14]. For simplicity, an ambient CO₂ concentration of 400 ppm was assumed. High air quality is assumed if both CO₂ readings were below 950 ppm. For concentrations between 950 ppm and 1200 ppm air quality is considered sufficient. High pollution with an immediate need for ventilation is assumed if the CO₂ concentration exceeds 1200 ppm. The higher CO₂ reading is used for classification if both sensors are connected.

The current temperature, humidity, IAQ, CO₂ (SCD30), CO₂ equivalent (BSEC) and the overall air quality assessment are shown on a 4.3" TFT display, as shown in Figure 3. An acoustic alert is triggered if the air quality exceeds a critical limit. The local display should motivate the people

to periodically air the room. That way, the CO₂ concentration and thus also the expose of potentially infectious aerosols can be kept below a critical level.

B. Online Display

The buffered sensor data is transmitted to an MQTT broker using the ESP32 Wi-Fi modem every 30 seconds. For the air quality display application, the data is stored in an InfluxDB time-series database [16]. The stored data sets can be displayed on a web dashboard using Grafana [17]. The actual CO₂ measurements and the CO₂ equivalent estimations from the VOC measurements over a period of 4 days are shown in Figure 4.

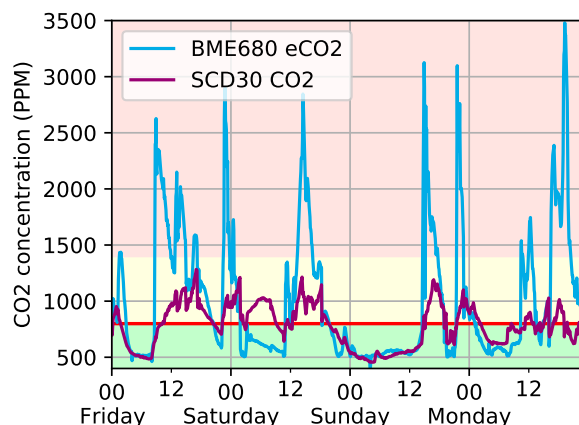


Fig. 4. Recorded actual (SCD30) and VOC based estimated (BME680) CO₂ concentration

In the event of a revealed Covid infection, the recorded data is possibly useful for a more accurate risk assessment to prevent a further spread of the virus.

C. CO₂ equivalent estimation

The NDIR CO₂ sensors are significantly more expensive compared to the VOC sensors. The estimated CO₂ equivalent from the BSEC sensor fusion is based on the assumption of the presence of human breath only. For other sources of CO₂, the estimation will usually be too small, as shown in Figure 4 for the time between Saturday midnight and noon. The gas resistance measurement is sensitive to a wide range of VOCs. Outgassing from furniture [18], detergents [19] or personal care products [22] results in a higher total VOC concentration, causing too high CO₂ estimates. The spikes for the CO₂ estimations in Figure 4 likely result from such effects. The cheap VOC sensor is therefore not capable of replacing the actual NDIR sensor if accurate CO₂ concentration values are required. For the use in an air quality display, the sensor could be suitable nevertheless because the readings determined are usually too high if other VOC pollutants are present. In this case, the airing of the room would be recommended anyway. Especially, if a larger number of sensors nodes should be deployed in large buildings to support air purity and ventilation, a significant price advantage of the BME680 becomes obvious.

IV. SPATIAL CO₂ CONCENTRATION

Objective of the proposed SN is the reduction of aerosol concentration indoors by indicating high CO₂ concentrations. In case of detection of high CO₂ concentration, room ventilation should be performed for a specific time. But the structure of a room and the localisation of windows and doors affect the aerosol distribution [21] and therefore the efficiency of ventilation in terms of local reduction of aerosol concentrations. As solution, multiple sensor nodes can be deployed to measure the CO₂ concentration at different locations inside a room. The use of multiple SNs helps to measure aerosol concentration in badly ventilated room corners and regions away from a window to optimize the ventilation frequency and duration and therefore to lower the aerosol concentration in all parts of a room. Theoretically, it is also possible to estimate the indoor aerosol distribution by mathematically modeling [20], but this is too complex for the proposed application, especially when equipping several rooms with sensor nodes. As experimental approach, multiple sensor nodes have been placed at different locations inside a room to get the spatial CO₂ concentration. The measured data was used to visualize and evaluate the air exchange during ventilation in order to optimize the ventilation process. This set-up could further be used to determine the optimal location for a single air quality display in typical room structures.

A. Experimental Setup

Due to the current Covid situation, it was not possible to perform measurements under realistic conditions with many humans being in a room like a university lecture hall. Therefore, preliminary data was recorded in the home office with a limited area of 19 m². The layout of the room is shown in Figure 5. SN 1 is placed on a TV rack in front of the room. SN 2 is placed on the upper side of the desk near a window. SN 3 is located in the opposite direction of the desk. SN 4 is mounted in a nested corner of the room. SN 5 is located near the door. All sensors are placed at a height of 1.5 m to limit the interpolation to 2 dimensions. The experiment begins with the door and all windows closed in order to demonstrate the effect of ventilation.

The time between the shown measurements was determined experimental in a way to best demonstrate the effect of airing and the rise of CO₂ concentration after closing the window. First measurements of CO₂ concentrations are performed just before the door and window *a* are opened. After 30 seconds the next measurements are taken. The door and the window are closed after 5 minutes of open time and a last set of measurements are acquired after additional 5 minutes.

B. Interpolation

The measured CO₂ concentrations are interpolated on a plane, representing a cross-section of the room. One challenge of the spatial interpolation for this application is the limited number of supporting points. The few measurement locations are further not placed on a regular grid. Basic multivariate interpolation techniques, e.g., bilinear interpolation, rely on a

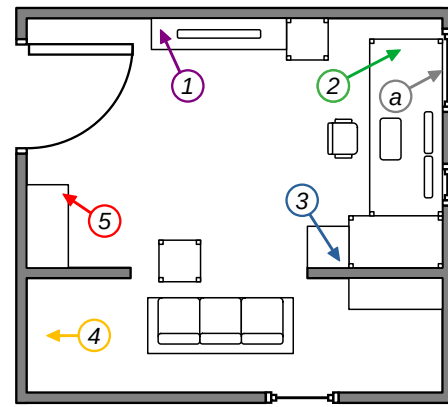


Fig. 5. Room layout with furniture, door, window (a) and position of 5 sensors

regular grid, which is why these methods are not suitable for this application [23]. Methods from geostatistics, e.g., kriging or inverse distance weighting (IDW) can be used with irregular distributed data. Kriging is a commonly used geostatistical approach assuming a spatial correlation between the sample points [24]. The data from the five SNs is not sufficient to create a meaningful variogram. Therefore, the deterministic IDW approach was used for interpolation. The estimated value is calculated by the values and distances to all sampled points, as shown in Equation 1 [25]. The weighting of each sample point only depends on the distance raised to the power of μ , neglecting the unknown spatial correlation. The interpolation points can only take values between the minima and maxima of the support points.

$$F(x, y) = \begin{cases} \frac{\sum_{k=1}^N (\frac{1}{d_k})^\mu f_k}{\sum_{k=1}^N (\frac{1}{d_k})^\mu} & \text{if all } d_k \neq 0 \\ f_k & \text{if any } d_k = 0 \end{cases} \quad (1)$$

F = Estimation for coordinate x, y

N = Number of samples

d_k = Distance between estimation and sample

μ = Power, determines the smoothing

f_k = Sample value

C. Results

Figure 6 shows the spatial CO₂ concentration at a height of 1.5 m before the experiment is started. The CO₂ concentration is almost identical at all measuring points (1416-1466 ppm) except for position 1 that is located near the door with 1239 ppm. Fresh air flowing through the gap underneath the door could explain the drop in CO₂ concentration at this sampling point.

The measurements recorded 30 seconds after opening the door and window *a* are shown in Figure 7. Fresh air is flowing through window *a* in direction of the door. The CO₂ concentration near the window is 468 ppm whereas in the corner of the room at position 4 still 1302 ppm is measured. Shortly after the start of airing, a concentration drop is visible

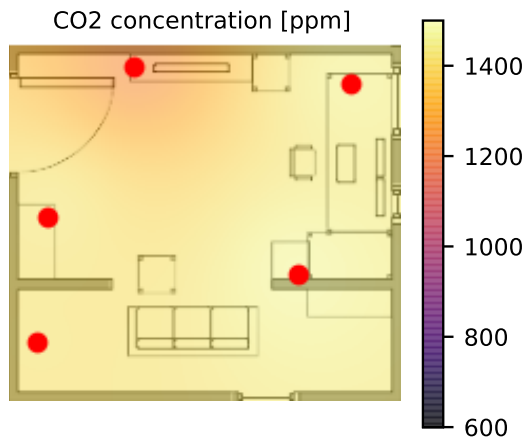


Fig. 6. Spatial CO2 concentration just before airing ($t = 0$)

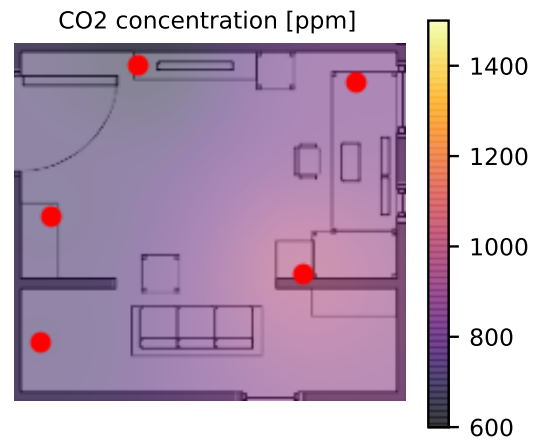


Fig. 8. Spatial CO2 concentration 5 minutes after the end of airing, i.e., at time $t = (5 + 5)$ min

in the direction of the window. The sensor readings measured at position 2 near the window are also fluctuating while the window is open. The airing results in a noticeable pulsating airflow near the window, causing a temporal variation of CO2 concentration near the window. Total airing time is 5 minutes.

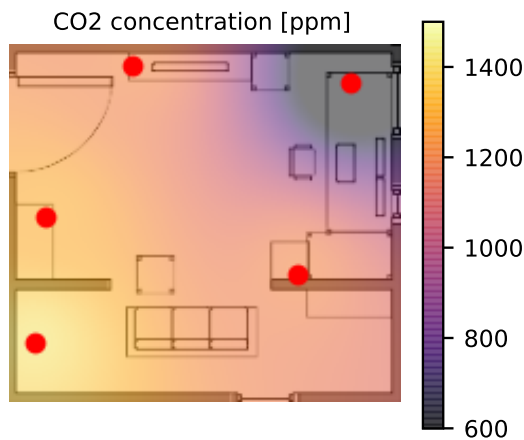


Fig. 7. Spatial CO2 concentration after ($t = 30$ s) seconds airing

The last measurements taken 5 minutes after the window a and the door were closed are shown in Figure 8. The CO2 concentration now settles between 664 ppm at position 1 near the door and 983 ppm at position 3 at the corner of the desk. The measurement at position 2 in the opposite direction of the desk near the window is 839 ppm. The CO2 concentration in the immediate environment of the workplace is already increasing after a short time when working at this place. To have an efficient result of the ventilation, i.e., low CO2 concentration in all regions of a room, multiple sensor nodes should be used to get a detailed view of the CO2 distribution.

Here, a simple guideline should be developed where to place the sensors in the room for typical room structures. In the proposed scenarios the sensors are wirelessly connected to a database. Future postprocessing of the recorded sensor data including visualization can be used to optimize number and position of sensors in a room. Result can be a guideline for e.g., facility managers to optimize SN deployment in different rooms and to reduce infection risk by keeping aerosol concentrations at reasonable low levels.

V. CONCLUSIONS

The deployment of the proposed air quality sensor with local display and alert functionality supports the ventilation habits to keep the room CO2 concentration below a critical limit. The online data logging could serve as an indicator for the infection risk in case of a detected Covid infection. The estimated CO2 equivalent from the BSEC sensor fusion is not as accurate as the directly measured value from the NDIR sensor but it is still sufficient as a rough indicator of the air quality. The BME680 sensor could be used for a low-cost variant of the sensor node, as the values are estimated rather too high. Due to the cost-efficiency of the SN, multiple of these nodes can be used in a single room to get a good view of spatial CO2 concentration.

The spatial distribution of the CO2 concentration as well as its dynamic change has been recorded in small room during an airing period. Right at the beginning of the airing a concentration gradient originating from the window was observed. In the direct vicinity of the workplace, an increased CO2 concentration is already detected shortly after the airing was stopped. From the preliminary data it can be concluded that the well-elaborated location of a single CO2 sensor inside the room is highly relevant. The positioning near doors and windows is not recommended because of possible draught resulting in too low measurement values not representing high CO2 concentrations as they may remain in isolated or nested regions of a room. If it is not possible to use multiple sensors, a single sensor should be placed further inside the room close

to the workplaces or in room corner with some distance to a window.

In future work, measurements have to be performed under real conditions in crowded lecture rooms and halls. Due to the current Covid restrictions, experiments under those conditions were not possible so far. It has to be analyzed how many sensor nodes should be used for typical room structures in order to have a cost-efficient but still safe solution to measure CO₂ concentration as basis to start the ventilation process. A planning tool could be developed that automatically calculates the number and positioning of sensor nodes inside a room. Database for this approach is the recorded sensor data captured in the planning phase when for a set-up time more nodes than required are used in a room to get sufficient sensor data from different regions of a room. As part of this planning tool, the interpolation quality has to be analyzed. The adjusted inverse distance weighting (AIDW) interpolation could be used to account for shielding effects resulting from space-dividing elements [26]. Furthermore, the used IDW approach could be compared to other interpolation techniques (e.g., radial basis functions [27]) to determine the best fitting method for spatial distribution of CO₂ in occupied space. The final planning tool can be an interactive graphical tool representing room structure and placement of sensors and optionally extended by dynamic sensor data visualization for analysis options.

REFERENCES

- [1] A. Hartmann and M. Kriegel, "Risk assessment of aerosols loaded with virus based on CO₂-concentration," *Preprint*, Jul. 2020, doi: 10.14279/DEPOSITONCE-10362.3.
- [2] Z. Ma, P. Cooper, D. Daly, and L. Ledo, "Existing building retrofits: Methodology and state-of-the-art," *Energy and Buildings*, vol. 55, pp. 889–902, Dec. 2012, doi: 10.1016/j.enbuild.2012.08.018.
- [3] N. Mahyuddin, H. B. Awbi, and M. Alshitawi, "The spatial distribution of carbon dioxide in rooms with particular application to classrooms," *Indoor and Built Environment*, vol. 23, no. 3, pp. 433–448, May 2014, doi: 10.1177/1420326X13512142.
- [4] P. Bolte, U. Witkowski, and R. Morgenstern, "Open Lorawan Sensor Node Architecture for Agriculture Applications," *3rd International Conference on Internet of Things (CIoT 2021)*, Sept. 2021, Canada, accepted for publication.
- [5] A. Bulińska, Z. Popiolek, and Z. Buliński, "Experimentally validated CFD analysis on sampling region determination of average indoor carbon dioxide concentration in occupied space," *Building and Environment*, vol. 72, pp. 319–331, Feb. 2014, doi: 10.1016/j.buildenv.2013.11.001.
- [6] J. Hodgkinson, R. Smith, W. O. Ho, J. R. Saffell, and R. P. Tatam, "Non-dispersive infra-red (NDIR) measurement of carbon dioxide at 4.2 μm in a compact and optically efficient sensor," *Sensors and Actuators B: Chemical*, vol. 186, pp. 580–588, Sep. 2013, doi: 10.1016/j.snb.2013.06.006.
- [7] Sensirion, "CO₂, humidity, and temperature sensor," SCD30 datasheet, Rev. 1.0, May 2020. Accessed Jun. 08, 2021. [Online]. Available: <https://www.sensirion.com/de/download-center/kohlendioxidensensoren-co2/co2-sensor>.
- [8] T. Lin, X. Lv, Z. Hu, A. Xu, and C. Feng, "Semiconductor Metal Oxides as Chemoresistive Sensors for Detecting Volatile Organic Compounds," *Sensors*, vol. 19, no. 2, p. 233, Jan. 2019, doi: 10.3390/s19020233.
- [9] D. A. Krawczyk, A. Rodero, K. Gładyszewska-Fiedoruk, and A. Gajewski, "CO₂ concentration in naturally ventilated classrooms located in different climates—Measurements and simulations," *Energy and Buildings*, vol. 129, pp. 491–498, Oct. 2016, doi: 10.1016/j.enbuild.2016.08.003.
- [10] Bosch, "Low power gas, pressure, temperature & humidity sensor," BME680 datasheet, Rev. 1.6, Jan. 2021. Accessed Jun. 08, 2021. [Online]. Available: <https://www.bosch-sensortec.com/media/boschsensortec/downloads/datasheets/bst-bme680-ds001.pdf>.
- [11] Bosch, "Integration Guide," Bosch software Environmental Cluster (BSEC), Jun. 2020. Accessed Jun. 08, 2021. [Online]. Available: <https://www.bosch-sensortec.com/software-tools/software/bsec/>.
- [12] "Nanopb - protocol buffers with small code size." <https://jpa.kapsi.fi/nanopb/> (accessed Jun. 08, 2021).
- [13] *Energetische Bewertung von Gebäuden - Lüftung von Gebäuden - Teil 1: Eingangsparameter für das Innenraumklima zur Auslegung und Bewertung der Energieeffizienz von Gebäuden bezüglich Raumluftqualität, Temperatur, Licht und Akustik - Modul M1-6*, DIN EN 16798-1:2021-04, Deutsches Institut für Normung, Berlin, Germany, Apr. 2021.
- [14] "Carbon dioxide levels continue at record levels, despite COVID-19 lockdown," World Meteorological Organization, Nov. 20, 2020. <https://public.wmo.int/en/media/press-release/carbon-dioxide-levels-continue-record-levels-despite-covid-19-lockdown> (accessed Jun. 08, 2021).
- [15] "InfluxDB contains everything you need in a time series data platform in a single binary" <https://www.influxdata.com/products/influxdb> (accessed Jun. 08, 2021).
- [16] "InfluxDB key concepts" <https://docs.influxdata.com/influxdb/v2.0/reference/key-concepts> (accessed Jun. 08, 2021).
- [17] "Grafana Labs, 'Grafana Features'," [Online]. Available: <https://grafana.com/grafana/> (accessed Jun. 08, 2021).
- [18] R. Menghi, S. Ceccacci, A. Papetti, M. Marconi, and M. Germani, "A method to estimate the total VOC emission of furniture products," *Procedia Manufacturing*, vol. 21, pp. 486–493, Jan. 2018, doi: 10.1016/j.promfg.2018.02.148.
- [19] W. W. Nazaroff and C. J. Weschler, "Cleaning products and air fresheners: exposure to primary and secondary air pollutants," *Atmospheric Environment*, vol. 38, no. 18, pp. 2841–2865, Jun. 2004, doi: 10.1016/j.atmosenv.2004.02.040.
- [20] T. Hussein and M. Kulmala, "Indoor Aerosol Modeling: Basic Principles and Practical Applications," *Water Air Soil Pollut: Focus*, vol. 8, pp. 23–34, 2008, <https://doi.org/10.1007/s11267-007-9134-x>.
- [21] I. Salma *et al.*, "Physical properties, chemical composition, sources, spatial distribution and sinks of indoor aerosol particles in a university lecture hall," *Atmospheric Environment*, vol. 64, pp. 219–228, 2013, <https://doi.org/10.1016/j.atmosenv.2012.09.070>.
- [22] A. M. Yeoman *et al.*, "Simplified speciation and atmospheric volatile organic compound emission rates from non-aerosol personal care products," *Indoor Air*, vol. 30, no. 3, pp. 459–472, 2020, doi: <https://doi.org/10.1111/ina.12652>.
- [23] E. J. Kirkland, *Advanced computing in electron microscopy*, Second edition. New York: Springer, 2010.
- [24] M. A. Oliver and R. Webster, "A tutorial guide to geostatistics: Computing and modelling variograms and kriging," *CATENA*, vol. 113, pp. 56–69, Feb. 2014, doi: 10.1016/j.catena.2013.09.006.
- [25] H. Hagen and D. Roller, *Geometric Modeling: Methods and Applications*. Berlin, Heidelberg: Springer Berlin Heidelberg, 1991.
- [26] Z. Li, K. Wang, H. Ma, and Y. Wu, "An Adjusted Inverse Distance Weighted Spatial Interpolation Method," in *Proc. 3rd Int. Con. Communications, Information Management and Network Security*, Nov. 2018, pp. 128–132, doi: 10.2991/cimns-18.2018.29.
- [27] M. Buhmann and J. Jäger, "On radial basis functions," *Snapshots of modern mathematics*, p. 02, 2019, doi: 10.14760/SNAP-2019-002-EN.